

ADA 082830

LINE 1
12
B.S.

RADC-TR-79-328

Interim Report

March 1980



ANALYSIS OF ADVANCED CI APPLICATIONS AND SYSTEMS PERFORMANCE

Optical Sciences Company

Sponsored by
Defense Advanced Research Projects Agency (DoD)
ARPA Order No. 2646

APPROVED FOR PUBLIC RELEASE; DISTRIBUTION UNLIMITED

DTIC
ELECTE
S APR 8 1980

A

The views and conclusions contained in this document are those of the authors and should not be interpreted as necessarily representing the official policies, either expressed or implied, of the Defense Advanced Research Projects Agency or the U. S. Government.

FILE COPY
DDC

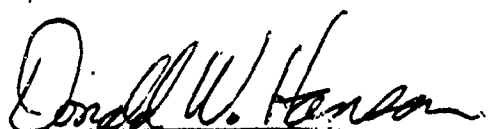
ROME AIR DEVELOPMENT CENTER
Air Force Systems Command
Griffiss Air Force Base, New York 13441

80 4 8 008

This report has been reviewed by the RADC Public Affairs Office (PA) and is releasable to the National Technical Information Service (NTIS). At NTIS it will be releasable to the general public, including foreign nations.

RADC-TR-79-328 has been reviewed and is approved for publication.

APPROVED:



DONALD W. HANSON
Project Engineer

If your address has changed or if you wish to be removed from the RADC mailing list, or if the addressee is no longer employed by your organization, please notify RADC (OCSE) Griffiss AFB NY 13441. This will assist us in maintaining a current mailing list.

Do not return this copy. Retain or destroy.

ANALYSIS OF ADVANCED CI APPLICATIONS AND SYSTEMS PERFORMANCE

David L. Fried
Stephen L. Browne

Contractor: Optical Sciences Company
Contract Number: F30602-79-C-0062
Effective Date of Contract: 20 March 1979
Contract Expiration Date: 30 September 1980
Short Title of Work: Analysis of Advanced CI
Applications

Program Code Number: 9E20
Period of Work Covered: Mar 79 - Oct 79

Principal Investigator: Dr. David L. Fried
Phone: 714 524-3622

Project Engineer: Donald W. Hanson
Phone: 315 330-3144
AV 587-3144

Approved for public release; distribution unlimited.

This research was supported by the Defense Advanced Research Projects Agency of the Department of Defense and was monitored by Donald W. Hanson (OCSE), Griffiss AFB NY 13441 under Contract F30602-79-C-0062.

UNCLASSIFIED

SECURITY CLASSIFICATION OF THIS PAGE (When Data Entered)

19 REPORT DOCUMENTATION PAGE		READ INSTRUCTIONS BEFORE COMPLETING FORM
1. REPORT NUMBER 18 RADC TR-79-328	2. GOVT ACCESSION NO.	3. RECIPIENT'S CATALOG NUMBER
4. TITLE (including subtitle) 6 ANALYSIS OF ADVANCED CI APPLICATIONS AND SYSTEMS PERFORMANCE	9	5. TYPE OF REPORT & PERIOD COVERED Interim Report Mar 79 - Oct 79
7. AUTHOR(s) 10 David L. Fried Stephen L. Browne	14	6. PERFORMING ORG. REPORT NUMBER DR-150
8. PERFORMING ORGANIZATION NAME AND ADDRESS Optical Sciences Company P O Box 446 Placentia CA 92670	15	7. CONTRACT OR GRANT NUMBER(s) F30602-79-C-0062 VARPA Order-2646
11. CONTROLLING OFFICE NAME AND ADDRESS Defense Advanced Research Projects Agency 1400 Wilson Blvd Arlington VA 22209	16	10. PROGRAM ELEMENT, PROJECT, TASK AREA & WORK UNIT NUMBERS 62301E 26460411
14. MONITORING AGENCY NAME & ADDRESS (if different from Controlling Office) Rome Air Development Center (OCSE) Griffiss AFB NY 13441	11	11. REPORT DATE March 1980
15. SECURITY CLASS. (of this report) UNCLASSIFIED	12	13. NUMBER OF PAGES 29
16. DISTRIBUTION STATEMENT (of this Report) Approved for public release; distribution unlimited.	31	15a. DECLASSIFICATION/DOWNGRADING SCHEDULE N/A
17. DISTRIBUTION STATEMENT (of the abstract entered in Block 20, if different from Report) Same		
18. SUPPLEMENTARY NOTES RADC Project Engineer: Donald Hanson (OCSE)		
19. KEY WORDS (Continue on reverse side if necessary and identify by block number) Atmospheric Optics Turbulence Adaptive Optics	Resolution Short Exposure Speckle Interferometry	
20. ABSTRACT (Continue on reverse side if necessary and identify by block number) In this report, two problems are considered. Chapter 1 examines the first problem, which is that of scaling previously developed probabilities of a good short exposure to other resolution conditions. Chapter 2 treats the second problem of combining low resolution adaptive optics with speckle techniques.		
In Chapter 1 results previously developed for the probability that at some instant the random wavefront distortion over a circular aperture will be less than one radian squared (averaged over the aperture at that instant) are		

UNCLASSIFIED

SECURITY CLASSIFICATION OF THIS PAGE(When Data Entered)

→ extended to apply to other values than one radian squared. These probabilistic results are then combined with estimates of the relationship between short exposure resolution and residual wavefront error to provide results for the probability of achieving some desired resolution as a function of aperture diameter. It is found that the optimum aperture diameter to achieve a desired level of resolution is almost exactly twice the diameter for which the diffraction limited resolution is equal to the desired resolution, and that the probability of obtaining the desired resolution with that aperture diameter is equal to the probability, previously evaluated, of having one radian squared residual wavefront error on a single short exposure with that aperture diameter. The ~~second part develops~~

→ The technique of stellar speckle interferometry has demonstrated such significant improvement in optical resolution over conventional imagery when viewing through a turbulent atmosphere, that one is prompted to suggest the possibility of introducing adaptive optics to the interferometric system for still further improvements in performance. In particular, since a high performance adaptive optics system would allow achievement of diffraction-limited performance by itself, we have considered the possible use of a coarse adaptive optics system, i.e., one with "excessively" large actuator elements in conjunction with speckle interferometry. To evaluate this possibility, in Chapter 2 we develop an expression for the power spectrum of the focal plane intensity in an adaptive optics two aperture (i.e., Michelson stellar interferometer) system acting on a turbulence-distorted single-point-source wavefront. The adaptive optics elements for this system are assumed to correspond to each single aperture of this two aperture system. It is found that no improvement in performance is achieved in speckle interferometry with adaptive optics over conventional optics, in as much as the power spectrum is virtually unchanged.

UNCLASSIFIED

SECURITY CLASSIFICATION OF THIS PAGE(When Data Entered)

PREFACE

This report is submitted in accordance with the requirements of Contract No. F30602-79-C-0062. It represents the results of work completed between March 1979 and October 1979.

This report is a collection of several reports which previously had been issued only informally. They are assembled in this document, each constituting a single chapter.

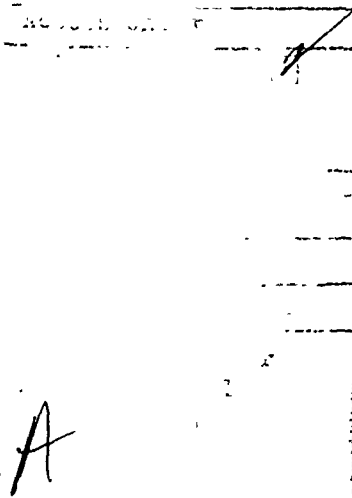


TABLE OF CONTENTS

<u>Chapter</u>	<u>Section</u>	<u>Title</u>	<u>Page</u>
1		Probabilistic Considerations for Instantaneous Wavefront Distortion Samples and for Short Exposure Resolution	1
	1.1	Analysis	2
	1.2	References for Chapter 1	12
2		Analysis of Speckle Interferometry as Applied to Adaptive Optics	13
	2.1	Introduction	14
	2.2	Analysis	15
	2.3	Conclusions	22
	2.4	References for Chapter 2	23

LIST OF FIGURES

<u>Figure No.</u>	<u>Title</u>	<u>Page</u>
1	Probability of Various Levels of Instantaneous Tilt-Free Aperture Averaged (RMS) Wavefront Distortion.	5
2	Dependence of $\Psi(\alpha)$ on α .	9
3	Probability of Achieving the Desired Resolution, R , As a Function of Aperture Diameter, D .	10

LIST OF TABLES

<u>Table No.</u>	<u>Title</u>	<u>Page</u>
1	Values of $\Psi(\alpha)$, Calculated from Eq. (18)	8
2	Probability of Achieving the Resolution R With an Aperture of Diameter, D .	10

Chapter 1

Probabilistic Considerations for
Instantaneous Wavefront Distortion Samples
and for Short Exposure Resolution

1.1 Analysis

In a recent paper¹ we calculated the probability that at any instant of time the squared wavefront distortion, (excluding the part of the distortion accountable as wavefront tilt) would be less than one radian-squared averaged over a circular aperture of diameter D . We showed that if the turbulence limited coherence diameter² were r_0 then the probability was well approximated by the expression

$$\text{Prob}(\mu^2 \leq 1 ; D, r_0) \approx 5.6 \exp[-0.1557 (D/r_0)^2] . \quad (1)$$

Here we have used the notation μ^2 to denote the aperture averaged squared (but tilt-free) wavefront distortion, measured in units of radians-squared. In this chapter we wish to extend this result to apply for other values of μ^2 than one radian-squared, and then to consider the probability of achieving various levels of resolution for different values of aperture diameter, taking account of the effect of the actual value of μ^2 on resolution.

We start by noting that the basis for development of Eq. (1) was the decomposition of the random wavefront distortion over the aperture area into a Karhunen-Loëve series with the random coefficient of the n^{th} term in the series having a mean value of zero and a variance σ_n^2 . It was shown that

$$\sigma_n^2 = \left(\frac{4}{\pi}\right)(D/r_0)^{5/3} B_n^2 , \quad (2)$$

where B_n is a parameter derived entirely from the five-thirds power dependence of the wave structure function and is dependent only on n . The second key to our analysis is to recall that Eq. (1) was obtained by noting that the probability in question corresponded to the probability

that an infinite set of zero mean gaussian random variables, $(S_1, S_2, S_3, \dots, S_n, \dots)$, with standard deviations, $(\sigma_1, \sigma_2, \sigma_3, \dots, \sigma_n, \dots)$, would have a sum of squared values, $(S_1^2 + S_2^2 + S_3^2 + \dots + S_n^2 + \dots)$ less than or equal to one. This probability relationship provided the equation

$$\text{Prob } (\mu^2 \leq 1; D, r_0) = \prod_{n=1}^{\infty} \int_{-1}^{1} dS_n (2\pi \sigma_n^2)^{-1/2} \times \exp(-\frac{1}{2} S_n^2 / \sigma_n^2) . \quad (3)$$

Here the notation L_1 denotes a composite limit for the multi-dimensional integral corresponding to a hyper-sphere of unit radius in the multi-dimensional space of $(S_1, S_2, S_3, \dots, S_n, \dots)$. This notation can be generalized to L_x denoting a hyper-sphere of radius x . Thus we can write, as a direct extension of the formulation that lead to Eq. (3), that the probability of μ^2 taking a value less than or equal to x^2 is given by the expression

$$\text{Prob } (\mu^2 \leq x^2; D, r_0) = \prod_{n=1}^{\infty} \int_{-x}^{x} dS_n (2\pi \sigma_n^2)^{-1/2} \times \exp(-\frac{1}{2} S_n^2 / \sigma_n^2) . \quad (4)$$

By a simple change of variables, with

$$s_n = S_n / x , \quad (5)$$

we can recast Eq. (4) in the form

$$\text{Prob } (\mu^2 \leq x^2; D, r_0) = \prod_{n=1}^{\infty} \int_{-1}^{1} ds_n [2\pi (\sigma_n/x)^2]^{-1/2}$$

$$x \exp[-\frac{1}{2} s_n^2/(\sigma_n/x)^2] . \quad (6)$$

Before attempting to exploit the form of Eq. (6), we first turn to a consideration of Eq. (1).

It is an easy matter to recast Eq. (1) in the form

$$(\sigma_n/x)^2 = \left(\frac{4}{\pi}\right) \left(\frac{D/x^{8/5}}{r_0}\right)^{5/3} s_n^2 . \quad (7)$$

Comparing Eq. (7) with Eq. (2) suggests that for a given value of r_0 , just as we would associate the value σ_n with the standard deviation of the n^{th} Karhunen-Loève series random coefficient for an aperture diameter D , we would associate the value σ_n/x with the standard deviation of the n^{th} random coefficient for an aperture diameter $D/x^{8/5}$. Now noting that the right-hand-side of Eq. (6) is equivalent to the right-hand-side of Eq. (3) except that σ_n in Eq. (3) is replaced by σ_n/x in Eq. (6), we see that we can equate the probability of μ^2 being less than or equal to x^2 for an aperture diameter D with the probability of μ^2 being less than or equal to unity for an aperture diameter of $D/x^{8/5}$. Thus, we can write

$$\text{Prob}(\mu^2 \leq x^2; D, r_0) = \text{Prob}(\mu^2 \leq 1; D/x^{8/5}, r_0) . \quad (8)$$

Now making use of Eq. (1) we can write

$$\text{Prob}(\mu^2 \leq x^2; D, r_0) = 5.6 \exp[-0.1557 x^{-12/5} (D/r_0)^2] . \quad (9)$$

This is the first of the results we seek. In Fig. 1 we show this probability plotted as a function of x for several different values of D/r_0 . The form of Eq. (9) suggests an interesting and rather simple test of our

theoretical results making use of short exposure astronomical observations with a fixed aperture telescope.

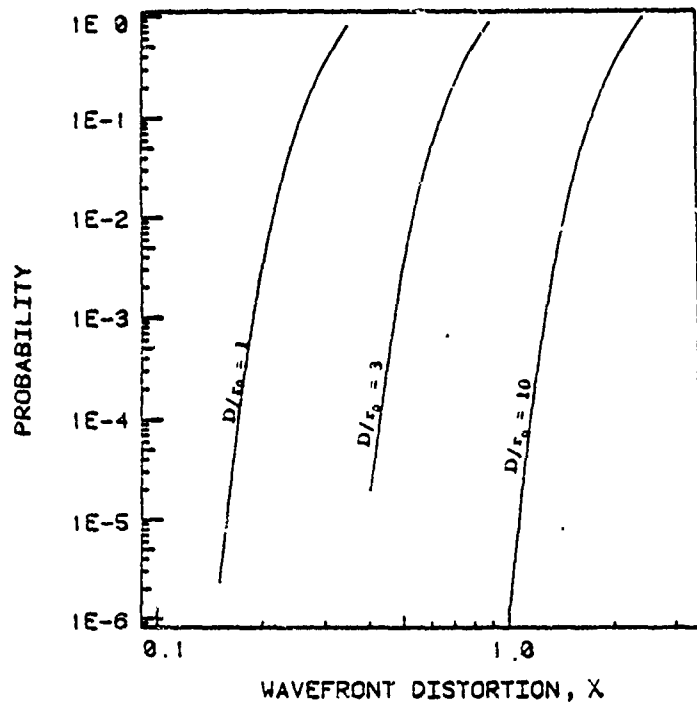


Figure 1. Probability of Various Levels of Instantaneous Tilt-Free Aperture Averaged (RMS) Wavefront Distortion.

Results are shown for three different values of aperture diameter, corresponding to $D/r_0 = 1, 3$, and 10 . Results shown here were calculated from Eq. (9). Wavefront distortion is measured in radians.

With Eq. (9) in hand we are now ready to turn to the second of the questions posed at the start of this note, i.e., what is the probability of achieving various levels of resolution with a particular aperture diameter, and as a corollary, what aperture diameter maximizes the probability of achieving a particular level of resolution. Following earlier procedures³ we define the resolution as the integral over spatial frequency of the wavefront distortion limited modulation transfer function of our aperture, $\tau(\vec{f})$, i.e., we can write the resolution as

$$R = \int d\vec{f} \tau(\vec{f}) . \quad (10)$$

It is convenient to reference this resolution to the long-exposure resolution achievable with a very large aperture diameter, which is limited by the coherence diameter, r_0 , and has the value³

$$R_0 = \int d\vec{f} \exp[-3.44(\lambda|\vec{f}|/r_0)^{5/3}] . \quad (11)$$

It can be shown that

$$R_0 = \frac{\pi}{4} \left(\frac{r_0}{\lambda} \right)^2 . \quad (12)$$

For a given aperture diameter, D , and instantaneous aperture average of the squared wavefront distortion, μ^2 , we wish to know what the resolution, R , is.

Strictly speaking, this value of R is a random variable which is not entirely determined by μ^2 (and D). However, if we note that we are actually interested in the expected value of R taken over the sub-ensemble of wavefront distortion samples which are characterized by this same value of μ^2 , then we can approximate that

$$R = \int d\vec{f} \tau_{0L}(\vec{f}; D) \exp[-3.44(\lambda|\vec{f}|/r_u)^{5/3}[1 - (\lambda|\vec{f}|/D)^{1/3}]] , \quad (13)$$

where r_u is a modified coherence diameter whose value is given by the expression

$$\mu^2 = \left(\frac{D}{3.40r_u} \right)^{5/3} , \quad (14)$$

so that

$$r_{\mu} = D \mu^{-8/5} / 3.40 \quad . \quad (15)$$

Eq. (14) is chosen in accordance with our previous analysis⁴ of the tilt-free aperture averaged wavefront distortion squared, so that r_{μ} will characterize a pseudo coherence diameter with ordinary wavefront distortion-like spatial characteristics but corresponding to an aperture averaged wavefront distortion squared of μ^2 , over an aperture of diameter D. $\tau_{0L}(\vec{f}; D)$ in Eq. (13) denotes the modulation transfer function associated with diffraction limited imaging through an aperture of diameter D. Its value is given by the expression

$$\tau_{0L}(\vec{f}; D) = \frac{2}{\pi} \left\{ \cos^{-1} \left(\frac{\lambda |\vec{f}|}{D} \right) - \left(\frac{\lambda |\vec{f}|}{D} \right) \left[1 - \left(\frac{\lambda |\vec{f}|}{D} \right)^2 \right]^{1/2} \right\} . \quad (16)$$

The form of Eq. (13) is based on the assumption (which we believe is plausible but not certain) that the samples of wavefront distortion characterized by some value of μ^2 have the same general spatial form as those characterized by any other value of μ^2 , but with a different scale factor—the scale factor being the modified coherence diameter, r_{μ} .

Combining these equations and appropriately simplifying, it can be shown that

$$R/R_0 = (D/r_0)^2 \Psi(\mu^2) \quad , \quad (17)$$

where the function $\Psi(\alpha)$ is defined by the equation

$$\Psi(\alpha) = 8 \int_0^1 x dx \left\{ \frac{2}{\pi} [\cos^{-1}(x) - x(1-x^2)^{1/2}] \right\}$$

$$x \exp [-26.45 (x^{5/3} - x^2) \alpha] . \quad (18)$$

In Table 1 we list some sample values of $\gamma(\alpha)$ and plot the function in Fig. 2.

TABLE I

Values of $\gamma(\alpha)$, Calculated From Eq. (18)

x	$\gamma(\alpha)$	α	$\gamma(\alpha)$	α	$\gamma(\alpha)$
.00	.99972	1.00	.30084	6.00	.020827
.05	.93619	1.25	.23226	6.25	.019616
.10	.87715	1.50	.18259	6.50	.018524
.15	.82229	1.75	.14616	6.75	.017536
.20	.77127	2.00	.11910	7.00	.016637
.25	.72383	2.25	.098720	7.25	.015817
.30	.67969	2.50	.083148	7.50	.015066
.35	.63862	2.75	.071075	7.75	.014376
.40	.60038	3.00	.061578	8.00	.013740
.45	.56478	3.25	.053997	8.25	.013151
.50	.53161	3.50	.047861	8.50	.012607
.55	.50071	3.75	.042827	8.75	.012101
.60	.47190	4.00	.038644	9.00	.011629
.65	.44503	4.25	.035127	9.25	.011190
.70	.41997	4.50	.032137	9.50	.010778
.75	.39658	4.75	.029571	9.75	.010393
.80	.37475	5.00	.027347	10.00	.010032
.85	.35436	5.25	.025404		
.90	.33530	5.50	.023694		
.95	.31749	5.75	.022179		

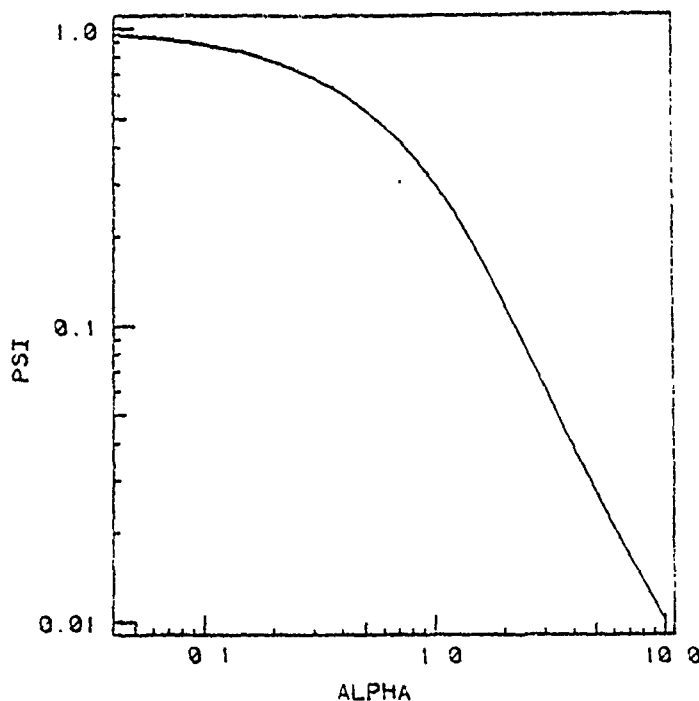


Figure 2. Dependence of $f(\alpha)$ on α .

The values plotted here are taken from Table 1. It is interesting to note that $f(\alpha)$ appears to be proportional to $\alpha^{-3/2}$ for values of α much larger than unity, and that it asymptotically approaches unity for very small values of α , with a knee in the curve of $\alpha \approx 0.5$.

We are now ready to calculate the probability of some desired level of resolution as a function of aperture diameter, D . We assume that r_0 is fixed and so our aperture diameter converts to a value for D/r_0 and our desired resolution converts to a value for R/R_0 . Then assuming some value for aperture diameter and making use of Eq. (17) and Table 1, we can solve for the allowed value of μ or rather of x . To achieve this level of resolution or better the aperture averaged squared tilt-free wave-front distortion, μ^2 , must have a value less than x^2 . The probability of this can be obtained by use of Eq. (9). Following this computational procedure we have prepared the data shown in Table 2 and plotted in Fig. 3. These represent our basic results for this chapter.

TABLE 2
Probability of Achieving the Resolution \bar{R} With an Aperture of Diameter D .

The quantity in parentheses accompanying each probability is the associated value of χ^2 , measured in radians-squared.

Diameter D/r_0	Probability			
	$R \geq 9 R_0$	$R \geq 16 R_0$	$R \geq 25 R_0$	$R \geq 36 R_0$
4	(0.45) 8.98×10^{-3}			
5	(0.84) 4.45×10^{-3}	(0.35) 5.69×10^{-4}		
6	(1.19) 5.80×10^{-4}	(0.65) 4.73×10^{-4}	(0.28) 4.89×10^{-11}	
7	(1.50) 5.04×10^{-5}	(0.93) 1.28×10^{-5}	(0.54) 5.30×10^{-7}	(0.24) 1.77×10^{-18}
8	(1.80) 4.10×10^{-6}	(1.19) 1.66×10^{-6}	(0.76) 5.85×10^{-8}	(0.45) 3.70×10^{-11}
9	(2.10) 3.14×10^{-7}	(1.43) 1.47×10^{-7}	(0.98) 1.30×10^{-8}	(0.65) 3.83×10^{-9}
10	(2.40) 2.35×10^{-8}	(1.66) 1.13×10^{-8}	(1.19) 1.71×10^{-8}	(0.84) 2.33×10^{-9}
11	(2.68) 1.75×10^{-9}	(1.88) 8.11×10^{-9}	(1.38) 1.53×10^{-8}	(1.01) 4.60×10^{-9}
12	(3.00) 1.31×10^{-9}	(2.10) 5.58×10^{-9}	(1.56) 1.11×10^{-8}	(1.19) 6.43×10^{-9}
13	(3.28) 1.00×10^{-9}	(2.32) 3.75×10^{-9}	(1.74) 7.25×10^{-9}	(1.35) 5.68×10^{-9}
14	(3.60) 7.86×10^{-10}	(2.53) 2.51×10^{-9}	(1.92) 4.98×10^{-9}	(1.50) 3.74×10^{-9}
15	(3.92) 6.22×10^{-10}	(2.75) 1.69×10^{-9}	(2.10) 3.13×10^{-9}	(1.66) 2.73×10^{-9}
16	(4.25) 4.98×10^{-10}	(2.98) 1.18×10^{-9}	(2.27) 1.84×10^{-9}	(1.80) 1.60×10^{-9}
17		(3.21) 8.28×10^{-10}	(2.45) 1.17×10^{-9}	(1.95) 9.48×10^{-9}
18		(3.44) 5.89×10^{-10}	(2.62) 7.31×10^{-9}	(2.10) 5.54×10^{-9}
19		(3.68) 4.26×10^{-10}	(2.80) 4.43×10^{-9}	(2.24) 2.90×10^{-9}
20		(3.92) 3.13×10^{-10}	(2.98) 2.75×10^{-9}	(2.39) 1.74×10^{-9}

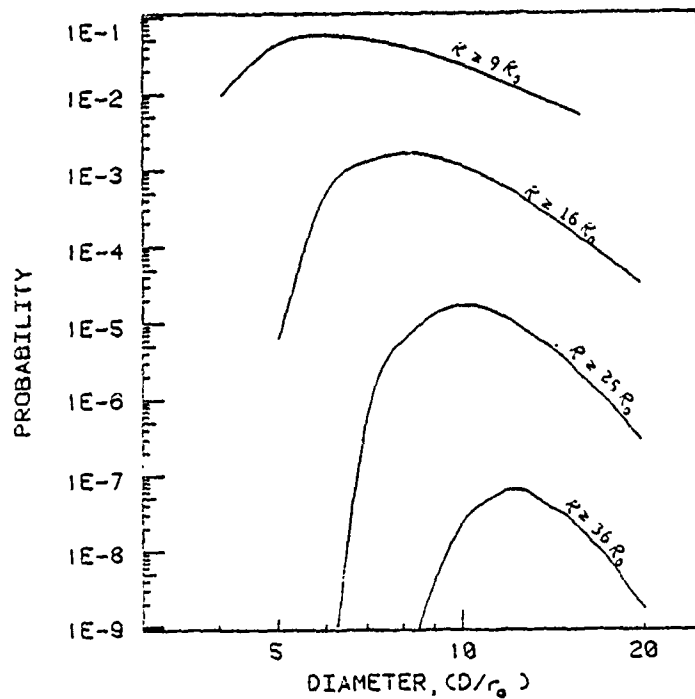


Figure 3. Probability of Achieving the Desired Resolution, \bar{R} , As a Function of Aperture Diameter, D .

The results plotted here are based on the data in Table 2.

Two things are worth noting from Table 2 and Fig. 3. First, we note that for any desired value of resolution, the maximum probability of achieving or exceeding this resolution is obtained if we choose an aperture diameter such that D/r_0 is equal to about $2(R/R_0)^{1/3}$. This means that the optimum aperture diameter for achieving a given resolution is twice the diameter that would just achieve that resolution with diffraction limited (i.e., turbulence-free) imaging. Second, we note that this maximum probability is achieved with an aperture averaged tilt-free wavefront distortion limit, χ^2 , of just about one radian-squared. This means that Eq. (1), our previously published result, adequately defines the probability of being able to achieve a given resolution if the aperture diameter is properly chosen to maximize the probability of achieving that resolution. It also allows us to write the probability of achieving a resolution R as

$$\text{Prob}(R \geq KR_0) \approx 5.6 \exp(-.6228 K) , \quad (19)$$

where K measures the factor better than turbulence limited imaging which we wish to achieve. It is also interesting to note that the probabilistic penalty of using a diameter larger than the optimum is small for the higher optimum probability cases, but becomes increasingly severe as we turn to the higher resolution lower optimum probability cases.

1.2. References for Chapter 1

1. D. L. Fried, "Probability of Getting a Lucky Short-Exposure Image Through Turbulence," *J. Opt. Soc. Am.* 68, 1651 (1978).
2. D. L. Fried, "Optical Heterodyne Detection of an Atmospherically Distorted Signal Wavefront," *Proc IEEE* 55, 57 (1967).
3. D. L. Fried, "Optical Resolution Through a Randomly Inhomogeneous Medium for Very Long and Very Short Exposures," *J. Opt. Soc. Am.* 56, 1372 (1966).
4. D. L. Fried, "Statistics of a Geometric Representation of Wavefront Distortion," *J. Opt. Soc. Am.* 55, 1427 (1965).

Chapter 2

Analysis of Speckle Interferometry

as

Applied to Adaptive Optics

2.1. Introduction

Although we wish to study the effect of speckle interferometry on large aperture adaptive optics, we will confine our analysis to the Michelson stellar with a single adaptive optics actuator corresponding to each of the two apertures, for the simple reason that it is mathematically and conceptually easy to do so, while the mathematics of a full circular aperture system appears intractable. We shall consider the adaptive optics to be a pair of discrete elements, one for each aperture, so that while the phase shift introduced by atmospheric turbulence varies over each element, the mean phase error of each element is removed, i.e., is equal to zero. It is clear that in a certain sense this pair of disjoint apertures case, corresponds to the disjoint pair of regions on a large circular aperture optical system which give rise to any particular spatial frequency in the focal plane. In this sense then the analysis of the Michelson stellar interferometer case may be equated with the analysis of a full aperture system for a particular spatial frequency. The principle difference between this analysis and the full aperture case is that in the latter we would have to consider many pairs of disjoint regions, each pair contributing to a particular focal plane spatial frequency of interest. To be mathematically exact we would have to take account of the rather limited correlation between these pairs of apertures. Because taking proper account of this correlation is mathematically very complex, while physically it appears that there should be no significant contribution to the final result, we have chosen to work with the much simpler problem of the adaptive optics version of the Michelson stellar interferometer.

2.2. Analysis

We consider the Labeyrie technique of speckle interferometry¹, with a single point source in our field-of-view at an angle $\vec{\theta}_0$. We assume that the source intensity, at wavelength λ , is such that the amplitude at our interferometer aperture is A . If we denote position on the aperture by the two-dimensional vector \vec{r} , and let $\phi(\vec{r})$ denote the instantaneous random phase shift at \vec{r} introduced by atmospheric turbulence, we may then write for the wave function at the aperture due to this point source

$$U(\vec{r}) = A \exp[i k \vec{\theta}_0 \cdot \vec{r} + i \phi(\vec{r})] , \quad (1)$$

where

$$k = 2\pi/\lambda , \quad (2)$$

is the optical wave number.

We assume that each element of the interferometer has a circular clear aperture with diameter, D . This allows us to introduce the function

$$W(\vec{r}) = \begin{cases} 1 & \text{if } \vec{r} \text{ falls within the aperture} \\ 0 & \text{otherwise} \end{cases} , \quad (3)$$

to provide a mathematical description of the aperture. Thus, the wave function of our point source as it appears in the focal plane, as a function of view-angle, is

$$u(\vec{\theta}) = \mathcal{U} \int d\vec{r} W(\vec{r}) \exp(-i k \vec{\theta} \cdot \vec{r}) U(\vec{r}) . \quad (4)$$

Here \mathcal{U} is a constant of proportionality that will drop out at our final results.

The focal plane intensity may be written as

$$I(\vec{\theta}) = \frac{1}{2} |u(\vec{\theta})|^2 . \quad (5)$$

In the Labeyrie technique, the quantities of interest are the fourier angular spatial frequency transform of the focal plane intensity,

$$S(\vec{f}) = \int d\vec{\theta} \exp(-2\pi i \vec{f} \cdot \vec{\theta}) I(\vec{\theta}) , \quad (6)$$

where \vec{f} is the spatial frequency (in units of cycles per radian), and the power spectrum,

$$J(\vec{f}) = \langle S^*(\vec{f}) S(\vec{f}) \rangle . \quad (7)$$

We use the angle bracket notation here and in the following to denote an ensemble average over all possible turbulence-induced wavefront distortion patterns.

Substituting Eq. (1) into Eq. (4), we get

$$u(\vec{\theta}) = U A \int d\vec{r} W(\vec{r}) \exp[i\phi(\vec{r}) - i k(\vec{\theta} - \vec{\theta}_0) \cdot \vec{r}] . \quad (8)$$

Substituting this into Eq. (5), and rewriting the product of integrals as a double integral, we get

$$I(\vec{\theta}) = \frac{1}{2} |U|^2 A^2 \iint d\vec{r} d\vec{r}' W(\vec{r}) W(\vec{r}') \times \exp \{ i[\phi(\vec{r}) - \phi(\vec{r}')] - i k[(\vec{\theta} - \vec{\theta}_0) \cdot (\vec{r} - \vec{r}')] \} . \quad (9)$$

Using Eq. (6), we may write for the spatial frequency fourier transform

$$\begin{aligned}
S(\vec{f}) = & \frac{1}{2} |\mathcal{U}|^2 A^2 \iiint d\vec{\theta} d\vec{r} d\vec{r}' W(\vec{r}) W(\vec{r}') \\
& \times \exp(-2\pi i \vec{f} \cdot \vec{\theta}) \exp\{i[\phi(\vec{r}) - \phi(\vec{r}')]\} \\
& - ik [(\vec{\theta} - \vec{\theta}_0) \cdot (\vec{r} - \vec{r}')] . \quad (10)
\end{aligned}$$

Replacing the variable of integration $\vec{\theta}$ by $\vec{v} = \vec{\theta} - \vec{\theta}_0$, we convert Eq. (10) to

$$\begin{aligned}
S(\vec{f}) = & \frac{1}{2} |\mathcal{U}|^2 A^2 \exp(-2\pi i \vec{f} \cdot \vec{\theta}_0) \iiint d\vec{v} d\vec{r} d\vec{r}' \\
& \times W(\vec{r}) W(\vec{r}') \exp\{i[\phi(\vec{r}) - \phi(\vec{r}')] - ik\vec{v} \cdot (\vec{r} + \lambda\vec{f} - \vec{r}')\} . \quad (11)
\end{aligned}$$

We may now use the well known property of fourier transforms, namely:

$$\iint dx dy' \exp[\pm 2\pi i x(y-y')] h(y') = h(y) , \quad (12)$$

to perform the \vec{v} - and \vec{r}' - integrations in Eq. (11). Thus, we obtain the result that

$$\begin{aligned}
S(\vec{f}) = & \frac{1}{2} |\mathcal{U}|^2 A^2 \exp(-2\pi i \vec{f} \cdot \vec{\theta}_0) \int d\vec{r} W(\vec{r}) W(\vec{r} + \lambda\vec{f}) \\
& \times \exp\{i[\phi(\vec{r}) - \phi(\vec{r} + \lambda\vec{f})]\} . \quad (13)
\end{aligned}$$

In developing this result we have absorbed a factor of λ^2 into the constant $|\mathcal{U}|^2$.

The power spectrum, $\mathcal{P}(\vec{f})$, is calculated by substituting Eq. (13) into Eq. (7). This results in the expression

$$\begin{aligned}
 \mathcal{J}(\vec{f}) &= \frac{1}{4} |\mathcal{U}|^4 A^4 \iint d\vec{r} d\vec{r}' W(\vec{r}) W(\vec{r} + \lambda \vec{f}) \\
 &\quad \times W(\vec{r}') W(\vec{r}' + \lambda \vec{f}) \langle \exp\{i[\phi(\vec{r}) - \phi(\vec{r}') \\
 &\quad + \phi(\vec{r}' + \lambda \vec{f}) - \phi(\vec{r} + \lambda \vec{f})]\} \rangle \quad . \quad (14)
 \end{aligned}$$

Here we have made a double integral out of the product of integrals so as to be able to write our result in this form.

To reduce this formidable expression, we shall use two tricks. The first is the realization that for a gaussian random variable with zero mean, say x , and any constant α , the ensemble average of the exponential of their product reduces to

$$\langle \exp(\alpha x) \rangle = \exp\left(\frac{1}{2} \alpha^2 \langle x^2 \rangle\right) \quad . \quad (15)$$

The second trick is to make use of the algebraic identity

$$(a-b+c-d)^2 = (a-b)^2 - (a-c)^2 + (a-d)^2 + (b-c)^2 - (b-d)^2 + (c-d)^2 \quad . \quad (16)$$

Making use of Eq.(15), the ensemble average of the exponential in Eq. (14) may be rewritten as

$$\begin{aligned}
 &\langle \exp\{i[\phi(\vec{r}) - \phi(\vec{r}') + \phi(\vec{r}' + \lambda \vec{f}) - \phi(\vec{r} + \lambda \vec{f})]\}\rangle \\
 &= \exp\left\{-\frac{1}{2} \langle [\phi(\vec{r}) - \phi(\vec{r}') + \phi(\vec{r}' + \lambda \vec{f}) - \phi(\vec{r} + \lambda \vec{f})]^2 \rangle\right\} \quad . \quad (17)
 \end{aligned}$$

So far, the discussion has paralleled (in fact, has been contiguous with) the development presented in our earlier work² for a standard (i. e., non-adaptive) optical system. To direct the discussion specifically toward the

Michelson interferometer (with adaptive optics), we introduce the concept of an average phase shift for a particular aperture element. We define the average phase-shift, Q_i , for the i^{th} aperture element

$$Q_i = \frac{1}{a_i} \int d\vec{r} \phi(\vec{r}) ,$$

where a_i is the area of the aperture element, and the integral is taken over the area of the i^{th} element. The average phase difference between two disjoint aperture elements, i and i' , would be $Q_i - Q_{i'}$. Since a Michelson interferometer has only two elements, we may denote this phase difference as

$$\begin{aligned} \Delta Q &= Q_i - Q_{i'} \\ &= \frac{1}{a_i} \int d\vec{r} \phi(\vec{r}) - \frac{1}{a_{i'}} \int d\vec{r} \phi(\vec{r}) \quad , \end{aligned} \quad (18)$$

Because the aperture element is under adaptive control, $Q_i - Q_{i'}$, will remain constant in spite of time-varying turbulence-induced changes in the wavefront reaching the aperture.

Examining the definition of $W(\vec{r})$ in Eq. (3), we see that the integrand in Eq. (14) will have a nonzero value only if \vec{r} , $\vec{r} + \lambda\vec{f}$, \vec{r}' , and $\vec{r}' + \lambda\vec{f}$ all fall within one or the other of the two aperture elements. If $|\lambda\vec{f}|$ is small compared to an element diameter, it is possible for all of \vec{r} , \vec{r}' , $\vec{r} + \lambda\vec{f}$, and $\vec{r}' + \lambda\vec{f}$ to fall within the same element. In this case, the mean square phase shift in Eq. (17) becomes

$$\begin{aligned} &\langle [\phi(\vec{r}) - \phi(\vec{r}') + \phi(\vec{r}' + \lambda\vec{f}) - \phi(\vec{r} + \lambda\vec{f})]^2 \rangle \\ &= \langle [\phi(\vec{r}) - \phi(\vec{r}')]^2 \rangle - \langle [\phi(\vec{r}) - \phi(\vec{r}' + \lambda\vec{f})]^2 \rangle \end{aligned}$$

$$\begin{aligned}
& + \langle [\phi(\vec{r}) - \phi(\vec{r} + \lambda\vec{f})]^2 \rangle + \langle [\phi(\vec{r}') - \phi(\vec{r}' + \lambda\vec{f})]^2 \rangle \\
& - \langle [\phi(\vec{r}') - \phi(\vec{r} + \lambda\vec{f})]^2 \rangle + \langle [\phi(\vec{r}' + \lambda\vec{f}) - \phi(\vec{r} + \lambda\vec{f})]^2 \rangle \\
& = \mathcal{D}(\vec{r} - \vec{r}') - \mathcal{D}(\vec{r} - \vec{r}' - \lambda\vec{f}) + \mathcal{D}(\lambda\vec{f}) + \mathcal{D}(\lambda\vec{f}) \\
& - \mathcal{D}(\vec{r} - \vec{r}' + \lambda\vec{f}) + \mathcal{D}(\vec{r} - \vec{r}') \quad \text{for } |\vec{f}| \leq \lambda/D , \quad (19)
\end{aligned}$$

where $\mathcal{D}(\vec{p})$ is the wave-structure function, defined by the equation

$$\mathcal{D}(\vec{p}) = \langle [\phi(\vec{r} + \vec{p}) - \phi(\vec{r})]^2 \rangle . \quad (20)$$

If $|\lambda\vec{f}|$ is large compared to an element diameter, nonzero values of the integrand of Eq. (14) occur only if \vec{r} and \vec{r}' fall in one aperture element, and $\vec{r} + \lambda\vec{f}$ and $\vec{r}' + \lambda\vec{f}$ fall in the other. In this case, taking account of the adaptive optics, the mean square phase shift in Eq. (17) becomes

$$\begin{aligned}
& \langle [\phi(\vec{r}) - \phi(\vec{r}') + \phi(\vec{r}' + \lambda\vec{f}) - \phi(\vec{r} + \lambda\vec{f})]^2 \rangle \\
& = \langle [\phi(\vec{r}) - \phi(\vec{r}') + [\phi(\vec{r}' + \lambda\vec{f}) - \Delta\Omega] - [\phi(\vec{r} + \lambda\vec{f}) - \Delta\Omega]]^2 \rangle \\
& = \langle [\phi(\vec{r}) - \phi(\vec{r}')]^2 \rangle - \langle [\phi(\vec{r}) - [\phi(\vec{r}' + \lambda\vec{f}) - \Delta\Omega]]^2 \rangle \\
& + \langle [\phi(\vec{r}) - [\phi(\vec{r} + \lambda\vec{f}) - \Delta\Omega]]^2 \rangle + \langle [\phi(\vec{r}) - [\phi(\vec{r}' + \lambda\vec{f}) - \Delta\Omega]]^2 \rangle \\
& - \langle [\phi(\vec{r}') - [\phi(\vec{r} + \lambda\vec{f}) - \Delta\Omega]]^2 \rangle + \langle [[\phi(\vec{r}' + \lambda\vec{f}) - \Delta\Omega] - [\phi(\vec{r} + \lambda\vec{f}) - \Delta\Omega]]^2 \rangle \\
& = \langle [\phi(\vec{r}) - \phi(\vec{r}')]^2 \rangle - \langle [\phi(\vec{r}) - \phi(\vec{r}' + \lambda\vec{f})]^2 \rangle - \langle \Delta\Omega^2 \rangle \\
& - 2 \langle \Delta\Omega [\phi(\vec{r}) - \phi(\vec{r}' + \lambda\vec{f})] \rangle
\end{aligned}$$

$$\begin{aligned}
& + \langle [\phi(\vec{r}) - \phi(\vec{r} + \lambda\vec{f})]^2 \rangle + \langle \Delta Q^2 \rangle + 2 \langle \Delta Q [\phi(\vec{r}) - \phi(\vec{r} + \lambda\vec{f})] \rangle \\
& + \langle [\phi(\vec{r}') - \phi(\vec{r}' + \lambda\vec{f})]^2 \rangle + \langle \Delta Q^2 \rangle + 2 \langle \Delta Q [\phi(\vec{r}') - \phi(\vec{r}' + \lambda\vec{f})] \rangle \\
& - \langle [\phi(\vec{r}'') - \phi(\vec{r} + \lambda\vec{f})]^2 \rangle - \langle \Delta Q^2 \rangle - 2 \langle \Delta Q [\phi(\vec{r}'') - \phi(\vec{r} + \lambda\vec{f})] \rangle \\
& + \langle [\phi(\vec{r} + \lambda\vec{f}) - \phi(\vec{r} + \lambda\vec{f})]^2 \rangle \\
= & \langle [\phi(\vec{r}) - \phi(\vec{r}')]^2 \rangle - \langle [\phi(\vec{r}) - \phi(\vec{r}'' + \lambda\vec{f})]^2 \rangle \\
& + \langle [\phi(\vec{r}) - \phi(\vec{r} + \lambda\vec{f})]^2 \rangle + \langle [\phi(\vec{r}') - \phi(\vec{r}' + \lambda\vec{f})]^2 \rangle \\
& - \langle [\phi(\vec{r}'') - \phi(\vec{r} + \lambda\vec{f})]^2 \rangle + \langle [\phi(\vec{r} + \lambda\vec{f}) - \phi(\vec{r} + \lambda\vec{f})]^2 \rangle \\
= & \mathcal{D}(\vec{r} - \vec{r}') - \mathcal{D}(\vec{r} - \vec{r}'' - \lambda\vec{f}) + \mathcal{D}(\lambda\vec{f}) + \mathcal{D}(\lambda\vec{f}) \\
& - \mathcal{D}(\vec{r}' - \vec{r} - \lambda\vec{f}) + \mathcal{D}(\vec{r}' - \vec{r}) \quad \text{for } |\vec{f}| \gg \lambda/D . \quad (21)
\end{aligned}$$

We see that Eq.'s (19) and (21) are identical, so we need not concern ourselves with the limitations of $|\vec{f}|$ in each expression. We may then rewrite Eq. (14) as

$$\begin{aligned}
\mathcal{D}(\vec{f}) = & \frac{1}{4} |\mathcal{U}|^4 (A)^4 \iint d\vec{r} d\vec{r}' W(\vec{r}) W(\vec{r} + \lambda\vec{f}) W(\vec{r}') W(\vec{r}' + \lambda\vec{f}) \\
& \exp\{-\frac{1}{2} [\mathcal{D}(\vec{r} - \vec{r}') - \mathcal{D}(\vec{r} - \vec{r}'' - \lambda\vec{f}) + \mathcal{D}(\lambda\vec{f}) + \mathcal{D}(\lambda\vec{f}) \\
& - \mathcal{D}(\vec{r}' - \vec{r} - \lambda\vec{f}) + \mathcal{D}(\vec{r}' - \vec{r}')] \} . \quad (22)
\end{aligned}$$

Eq. (22) is identical to Eq. (18) of our previous work² which was developed under the assumption of stationary optics.

2.3. Conclusions

The logic used to develop Eq. (22) may be extended beyond the Michelson interferometer with two widely spaced aperture elements, to include any finite number of nonoverlapping aperture segments. Thus, we see that the introduction of adaptive optics has not at all affected the power spectrum of the focal plane intensity.

In other words, no improvement whatsoever can be expected from removing the average phase shift error from a pair of finite-sized disjoint elements in the aperture. It is only if the adaptive optics makes fine enough scale corrections for $\delta(\vec{r} - \vec{r}')$ to be affected for the small separations $|\vec{r} - \vec{r}'|$ that the adaptive optics could affect the power spectrum. For the very coarse form of adaptive optics which we are considering here, for which there is no adaptive optics correction of the wavefront distortion between two points \vec{r} and \vec{r}' close enough together to be in the same aperture element of the Michelson stellar interferometer, the adaptive optics cannot affect the statistical quality of the focal plane pattern. In this case, we see the speckle interferometry is not helped by use of coarse adaptive optics.

2.4. References for Chapter 2

1. A. Labeyrie, "Attainment of Diffraction Limited Resolution in Large Telescopes by Fourier Analysing Speckle Patterns in Star Images," *Astr. and Ap.*, 6, 85 (1970).
2. D. L. Fried, "Analysis of Techniques for Imaging through the Atmosphere," Interim Report RADC-TR-78-285, January 1979. (A066598)

MISSION
of
Rome Air Development Center

RADC plans and executes research, development, test and selected acquisition programs in support of Command, Control Communications and Intelligence (C³I) activities. Technical and engineering support within areas of technical competence is provided to ESD Program Offices (POs) and other ESD elements. The principal technical mission areas are communications, electromagnetic guidance and control, surveillance of ground and aerospace objects, intelligence data collection and handling, information system technology, ionospheric propagation, solid state sciences, microwave physics and electronic reliability, maintainability and compatibility.